CSIRO PUBLISHING

International Journal of Wildland Fire
https://doi.org/10.1071/WF18216

Exploring fire response to high wind speeds: fire rate of spread, energy release and flame residence time from fires burned in pine needle beds under winds up to 27 m s^{-1}

Bret Butler[A,E], *Steve Quarles*[B], *Christine Standohar-Alfano*[D], *Murray Morrison*[B], *Daniel Jimenez*[A], *Paul Sopko*[A], *Cyle Wold*[A], *Larry Bradshaw*[A], *Loren Atwood*[A], *Justin Landon*[A], *Joseph O'Brien*[C], *Benjamin Hornsby*[C], *Natalie Wagenbrenner*[A] and *Wesley Page*[A]

[A]US Forest Service, Rocky Mountain Research Station, Fire Fuel and Smoke Program, 5775 Highway 10 W, Missoula, MT 59802, USA.
[B]Insurance Institute for Business & Home Safety, 5335 Richburg Road, Richburg, SC 29729, USA.
[C]US Forest Service, Southern Research Station, Center for Forest Disturbance Science, 320 Green Street, Athens, GA 30602, USA.
[D]Haag Engineering, 10926 Quality Drive, Charlotte, NC 28278, USA.
[E]Corresponding author. Email: bwbutler@fs.fed.us

Abstract. The relationship between wildland fire spread rate and wind has been a topic of study for over a century, but few laboratory studies report measurements in controlled winds exceeding 5 m s^{-1}. In this study, measurements of fire rate of spread, flame residence time and energy release are reported for fires burning under controlled atmospheric conditions in shallow beds of pine needles subject to winds ranging from 0 to 27 m s^{-1} (measured 5 m above ground level). The data suggested that under constant flow conditions when winds are less than 10 m s^{-1}, fire rate of spread increases linearly at a rate of ~3% of the wind speed, which generally agrees with other laboratory-based models. When wind speed exceeds 10 m s^{-1}, the fire rate of spread response to wind remains linear but with a much stronger dependence, spreading at a rate of ~13% of the wind speed. Radiative and convective heating correlated directly to wind speed, with radiant heating increasing approximately three-fold as much as convective heating over the range of winds explored. The data suggested that residence time is inversely related to wind speed and appeared to approach a lower limit of ~20 s as wind exceeded 15 m s^{-1}. Average flame residence time over the range of wind speeds was nominally 26 s.

Additional keywords: empirical modelling, fire behaviour, high wind speeds.

Received 4 December 2018, accepted 1 October 2019, published online 21 November 2019

Introduction

Wildland fire rate of spread is dependent on many factors, one of which is the wind acting on the fire (Nelson and Adkins 1988). A fire burning in natural vegetation during calm wind conditions can dramatically increase in spread rate and intensity when exposed to even moderate winds. Although wind can tilt flames, resulting in more efficient heating of fuels ahead of the flame front, Potter (2012) notes that wind also enhances diffusion of oxygen to the combustion zone, which increases the chemical reaction rate, leading to increased energy output and rate of spread. Although the basic mechanisms that govern the effects of wind on wildland fire spread are well known, there is still significant uncertainty regarding the underlying physical processes at work (Finney *et al.* 2013). Wind-induced increases in fire spread and intensity have been linked to escaped prescribed fire incidents, extensive property damage and firefighter and public injury and deaths (Butler 2014). Adequate knowledge of the relationships between wind and fire spread rate and intensity are critically important because these relationships are incorporated into the fire spread models that are used for wildland fire management decision support throughout the world (Alexander *et al.* 2000; Lopes *et al.* 2002; Andrews *et al.* 2008; Sharples *et al.* 2012).

The wind speed versus fire rate of spread relationships presented in existing published studies for a range of fuel types vary from linear to exponential (Fang 1969; Rothermel 1972; Nelson and Adkins 1988; Wotton *et al.* 1999). Sullivan (2009) notes that the power law relationships presented from both laboratory- and field-based empirical models with exponents greater than unity are commonly used to fit data at low wind speeds, even though such functions will eventually result in spread rates greater than the wind speed unless they are constrained. In the early version of the Rothermel spread model (Rothermel 1972), a wind limit was imposed above which the fire rate of spread decreased with increasing wind based on data from Australia (McArthur 1966, 1969); however, this wind limit has since been removed from the version of the Rothermel model used for fire decision support in the USA (Andrews *et al.* 2013). Most laboratory studies focused on wind and fire spread relationships have been limited to wind speeds less than 5 m s^{-1}, except for a few observations from uncontrolled wildfires (McArthur 1966, 1969); thus, many of the published relationships may not be appropriate for high wind speed scenarios (Sullivan 2009).

Murphy (1963) and Murphy *et al.* (1966) studied fire spread over beds of wood flour in winds up to 4.47 m s^{-1} and slopes from zero to 50%. Maximum fire spread rate was 0.0012 m s^{-1} and results indicated little influence of slope on the rate of spread for the wind range explored. Rothermel and Anderson (1966) burned ponderosa pine (*Pinus ponderosa* Douglas ex C. Lawson) and western white pine needles (*P. monticola* Douglas ex D. Don) with a fine dead fuel moisture content of less than 5% at bed depths of 7.5 cm and 5 cm and fuel loadings of 2.45 kg m^{-2} and 1.61 kg m^{-2} respectively at winds from zero to 3.6 m s^{-1}. Results suggested an inverse linear relation between rate of spread and moisture content and a non-linear direct correlation with wind speed. Weise and Biging (1996) reported measurements of fire spread rate in a tilting open-top wind tunnel in which the fuel bed was 0.69 m wide and 2.52 m long at wind speeds up to 1.7 m s^{-1} and slopes ranging from –30% to +30%. Fuels were vertical sticks constructed of paper birch (*Betula papyrifera* Marshall) combined with a very thin layer of shredded aspen (*Populus tremuloides* Michx.) evenly distributed in a shallow layer along the floor of the fuel tray, with a fuel load and fuel bed depth of 0.56 kg m^{-2} and 11.4 cm respectively. Winds were generated by a fan located at the front edge of the fuel bed and fumes were exhausted through the open top (Weise 1994). Their data suggested a non-linear relationship for the dependence of rate of spread on wind speed. Catchpole *et al.* (1998) reported results from experiments conducted in a closed wind tunnel with controlled air temperature and humidity, burning both wood shavings and conifer needles from at least two species of softwoods for winds from 0 to 3.3 m s^{-1}. Their work exhibited a monotonically increasing correlation between fire rate of spread and wind speed over the range of winds explored. Mendes-Lopes *et al.* (2003) presented data from experiments conducted in a low speed wind tunnel with fuel beds of *P. pinaster* (Ait.) needles under winds from 0 to 3 m s^{-1} and slopes of –15% to +15%. Their results suggested that the rate of spread directly correlates with wind speed and that wind has a stronger effect on the rate of spread than does fuel moisture content. McArthur (1969) related fire rate of spread in natural fuels to average wind velocity over open terrain for winds as strong as 14.5 m s^{-1}. His data showed a direct relationship between fire rate of spread and wind speed up to a limit of 11 m s^{-1}, above which fire rate of spread decreased with increasing wind. Beer (1991, 1993) studied fires burning in winds up to 9.2 m s^{-1} and posited a power law relation with two regimes: one for winds less than 2.5 m s^{-1} and one for winds greater than 2.5 m s^{-1}. He proposed that the relative contribution of radiative and convective energy to the fire spread directly depended on wind speed. Beer (1991) evaluated the physics underlying fire–wind interaction and proposed that the three-dimensional nature of buoyant plumes above fires formed peaks and troughs that interact with local wind fields through complicated mechanisms that enhance energy transport to the unburned fuel ahead of the fire front. He surmised that fluctuations in wind speed enhance the fluctuations in flame shape, height and tilt angle, thereby enhancing advective heating of the fuels, which leads to increased spread rates. Finney *et al.* (2015) are exploring this theory further in controlled laboratory experiments.

In the present study the rate of spread, flame residence time and energy release from windblown fires burning over fuel beds of pine needles for wind speeds ranging from 0.4 to 27 m s^{-1} measured 5 m above ground level (AGL) were measured. A subset of experiments also explored how fire responds to laboratory-generated winds designed to replicate the variability in speed and direction of winds flowing over flat, open terrain. The experiments were conducted with three primary objectives: (1) extend the understanding of the dependence of fire rate of spread from laboratory experiments to higher wind speeds; (2) measure energy release from flames as a function of wind speed; and (3) explore the relationship between fire residence time and wind speed.

Methods

Experimental setup and facility

Burn experiments were conducted during June of 2016 at the Insurance Institute for Business & Home Safety (IBHS) located in Richburg, South Carolina, USA (Fig. 1). This facility includes a large wind tunnel (approximate footprint of experimental floor space is 44.2 × 44.2 m) that is able to generate average wind speeds between 5 and 58 m s^{-1} (Fig. 1*a*) and is designed with an array of active and passive elements for control of large- and small-scale turbulence in the wind field (Standohar-Alfano *et al.* 2017). These elements include: (1) an array of 105 fans (7 rows × 15 columns) each 1.8 m in diameter powered by a 350-horse power direct current electric motor with active speed control to generate large-scale gusts, (2) fixed passive spires in the lower and middle fan plenums, designed to introduce small-scale turbulence in the flow and (3) active wind vanes at the fan plenum exits that, when activated, induce lateral turbulence into the flow. It is intended that through these means the facility can replicate the turbulent spectra present in the atmospheric boundary layer (ABL) for flow over short, uniform vegetation and flat terrain. The facility was designed so that streamwise turbulence intensity in the generated wind field best matches that found in ABL flow at heights less than 5 m AGL. Measurements indicate that the facility is able to generate a velocity profile that replicates a theoretical logarithmic boundary layer profile with a roughness length $z_o = 0.01$ m. The passive spires are present at all times, which likely results in a difference in the turbulence spectra between the flow field in this facility and that found in a wind tunnel with constant fan speed and no passive or active turbulence generating capability.

For the data presented here, three flow types were explored: (1) fan speed and vane direction held constant to generate an average wind speed with a representative typical logarithmic boundary layer profile (termed flow type C), (2) a wind with induced fluctuations in the longitudinal wind speed, generated by modulating fan speeds, replicating a 1-Hz time history of wind

Fig. 1. (*a*) Exterior photo of fan array at the Insurance Institute for Business & Home Safety facility and (*b*) experimental chamber where staff are constructing fuel beds in preparation for a burn.

Table 1. Variables, symbols and units

Rate of fire spread	R	m s^{-1}
Wind speed measured at 5 m above ground level at the exit of the plenum	U_5	m s^{-1}
Wind speed measured at 28 cm above the fuel tray surface (20.4 cm above the upper surface of fuel) at 20 m along the length of the fuel bed	$U_{0.28}$	m s^{-1}
Fine dead fuel moisture content	M_f	% dry mass
Residence time	t_r	s
Flow type		
Constant wind speed and direction	C	–
Wind speed and direction varying in time	R	
Speed held constant but direction varies in time	RW	
Full dataset with all flow types and individual observations from each fuel bed	Full	–
Modified dataset consisting of only the burns with a constant wind flow type and the average characteristics (i.e. rate of spread and fuel moisture) of the two fuel beds during a burn	Mod	–
Modified dataset excluding burns where U_5 was <10 m s^{-1}	ModGr10	–
Modified dataset excluding burns where U_5 was ≥10 m s^{-1}	ModLe10	–

speed over open terrain but no directional variability imposed (flow type RW) and (3) a wind field with controlled fluctuations in both the longitudinal (speed) and lateral (direction) components (Standohar-Alfano *et al.* 2017) that generate a wind time history that exactly replicates a 1-Hz time history of speed and direction as well as the turbulence spectra of the ABL over open terrain (termed flow type R). Definitions for each of the dependent and independent variables are listed in Table 1.

Two parallel fuel trays, 3 m wide × 24 m long, were constructed on the floor of the IBHS facility (Fig. 1*b*). For the purposes of discussion they are referred to as the north and south fuel trays. The lateral adjacent edges of the trays were separated by ~3 m, with the long axis of the tray oriented parallel to the longitudinal axis of the wind flow. Regarding fuel tray width, Catchpole *et al.* (1998) argue that fuel beds must be at least 1 m wide and that the sides of the fuel beds should be designed to restrict inflow to the edges of the fuel array as well to reflect radiative heat back into the fuel array, thereby approximating a much wider array. Wotton *et al.* (1999) suggested that fire rate of spread is constant for flame widths greater than 2 m. Based on these two studies a bed width of 3 m was selected. The fuel trays consisted of a double layer of 1.58 cm thick × 244 cm long by 122 cm wide gypsum boards (total thickness 3.16 cm) placed on the floor of the tunnel with additional 8.9 cm tall, non-porous edges placed along the sides of each tray. Eleven burns were conducted under flow type C (i.e. constant wind speed and direction), five under flow type R (i.e. designed to replicate the turbulent spectra present in natural wind fields over open terrain), and one under flow type RW (i.e. varying direction but constant fan speed). For the final and highest speed experiment only one fuel bed was constructed, because of time constraints.

Wind speed was measured 5 m AGL at the plenum exit. For the purposes of this study, wind speeds for referenced studies were converted to those that would exist 5 m AGL based on a log wind profile and roughness factor of 0.0024 (http://wind-data.ch/tools/profile.php?lng=en, accessed 18 September 2017). When comparison was made to published datasets in which mid-flame winds were reported, but no flame or fuel height data were presented, the measurement height was assumed to be 1.0 m and a corresponding logarithmic conversion to 5 m AGL was made.

A common landscaping material in the south-eastern region of the USA consists of dead pine needles, primarily from slash (*P. elliottii* Engelm.) and longleaf (*P palustris* Mill.) pine trees, that are packaged in bales much like agricultural feed hay. This material is commonly referred to as 'pine straw'. Taking advantage of the availability of this material, a supply of pine straw bales was purchased and stored in a climate-controlled container 1 week before starting the burns. Immediately before each burn, the required quantity of bales was removed from storage, separated into weighed amounts and distributed on the fuel trays to a target fuel depth of 8.9 cm and packing ratio of 0.02. Fuel loading was nominally 0.84 kg m^{-2}, based on an assumed moisture content of 8%. Samples of fuels were collected immediately before ignition from nominally 3 m and 20 m along the longitudinal axis of each fuel bed to determine fuel moisture content following the standard oven-drying procedure (temperature between 100°C and 110°C for more than 24 h)

(Matthews 2010). Oven-dried moisture content was nominally 15% for burns 1 and 2, 12% for burn no. 3 and between 5% and 8% for all other burns.

Once the fuel beds were constructed and all preparations were complete, fans were set to the idle setting (~5 m s^{-1}). A propane burner consisting of a 3-m length of pipe with nominally 1-mm diameter holes drilled in the downwind edge was placed at the leading edge of each fuel bed. The burner was ignited manually using handheld propane torches. The propane flames quickly ignited the adjacent pine needles, creating a linear 3-m wide flame. As soon as the flame front was established and personnel had moved to a safe area, the fans were accelerated to the target wind speed. Time between flame presence and initial fan ramp up was less than 5 s. Time for fans to accelerate from idle to full speed was less than 3 s at the highest speeds and less than 2 s at lower speeds. After most burns were complete very little ash remained and any that was present was blown longitudinally along the fuel tray or was manually removed from the fuel tray.

Measurements

Fire rate of spread was characterised through analysis of overhead nadir-oriented video records. For this method, visible targets were placed on the edge of the fuel tray and on the floor between the fuel beds. These targets had a length designation as well as a unique identifier that was visible in the video image. Overall rate of spread was calculated as the average of the fire front transit time and travel distance between 5 and 24 m, 10 and 20 m and 15 and 24 m along the bed tray length, except for the zero wind burn where rate of spread was calculated as the time to spread from 0 to 3, 1 to 2 and 2 to 3 m.

Flame residence was calculated from overhead video records as the time for a specific location on the bed to complete flaming combustion. The beginning of flaming was defined by visual observation of the flame front arriving at a specific point along the fuel bed; the ending time was defined as that time at which the majority of flaming combustion was complete at the same location. For the highest wind speeds the partially burned fuel bed was blown down the fuel tray, essentially forming a secondary flaming and smouldering rolling flame front. In this case the flame residence time was not collected. Flame depth for each burn was calculated as the product of the measured residence time and the rate of spread.

Radiative and convective heating were measured for a subset of the burns by sensors located ~0.5 m above the floor surface at 5 m and 25 m along the longitudinal axis of the fuel tray. These sensors have been described elsewhere (Frankman *et al.* 2013*a*) and are designed to measure heating incident on the sensor as the flames approach and burn around the sensor. Sensors signals were recorded at 10 Hz. Based on the frequency analysis of Frankman *et al.* (2013*b*), reported values represent 3-s averages of the measured signal.

Analysis

Seven statistical models were developed based on four subsets of the data and two model forms to quantify the effect of wind speed and fuel moisture content on the rate of spread and to aid in comparisons with other existing empirical and quasi-empirical models (Sullivan 2009). The subsets of the data included (1) the full dataset with all flow types and individual observations from each fuel bed (Full, $n = 33$), (2) a modified dataset consisting of only the burns with a constant wind flow type and the average characteristics (i.e. rate of spread and fuel moisture) of the two fuel beds during a burn (Mod, $n = 12$), (3) the modified dataset excluding burns where U_5 was <10 m s^{-1} (ModGr10, $n = 8$) and (4) the modified dataset excluding burns where U_5 was ≥10 m s^{-1} (ModLe10, $n = 4$). These datasets were fit with two model forms: a non-linear functional form that incorporated a power function for wind speed and an exponential decay function for fine dead fuel moisture content (Cheney *et al.* 1998; Cruz *et al.* 2013; Anderson *et al.* 2015) (Eqn 1) and a simple linear model based on ordinary least-squares regression (Eqn 2). The *nls* and *lm* functions in the R software package (R Core Team 2014) were used to estimate the model coefficients for the non-linear and linear model forms, respectively. Note that Eqn 1 was not fit to the ModLe10 dataset because of inadequate sample size. The two model forms were:

$$R = aU_5^b \exp(-cM_f) \quad (1)$$

$$R = a + bU_5 - cM_f \quad (2)$$

where R is the rate of spread (m s^{-1}), a, b and c are model specific constants, U_5 is the wind speed at 5 m a.g.l. at the exit of the plenum (m s^{-1}) and M_f is the fine dead fuel moisture content (% dry mass). The goodness-of-fit statistics calculated for each model included the adjusted coefficient of determination for the linear models (R^2), and the root mean square error (RMSE) and mean absolute percent error (MAPE) following Willmott (1982). Akaike's information criterion (AIC) was also used to aid in comparing the relative suitability of models built using the same dataset (Akaike 1973).

An analysis of covariance (ANCOVA) was completed using the full dataset to determine if flow type had a significant effect on the laboratory measured R. The covariates of U_5 and M_f were included in the model to correct for the influence of different wind speeds and dead fuel moisture content encountered during each of the burns. The assumptions of homogeneity of variance and normality of the residuals were assessed using Levene's test (Levene 1960) and the Shapiro–Wilk normality test (Shapiro and Wilk 1965), respectively. Ordinary least-squares regression was also used to evaluate the strength of the linear relationships among peak radiative and convective heat fluxes with U_5 and R and the relative effects of wind speed on the measured convective and radiative heat fluxes. Additionally, Welch's two sample *t*-tests assuming unequal variances were used to assess differences in mean peak radiative and convective heat flux across increasing wind speed levels.

Results and discussion

Rate of spread and wind speed

The primary measured values for each burn are listed in Table 2 and basic descriptive statistics for the seven datasets used in the analysis are given in Table 3.

Fig. 2 compares the fire rate of spread as a function of wind speed for the entire dataset from these experiments to models presented by three laboratory-based studies that included at least

Table 2. Experimental conditions and key measurements for each burn

Fuel bed A corresponds to the north fuel bed and fuel bed B corresponds to the south fuel bed. Note that R and t_r represent the average values obtained from the nadir-oriented video records using transit times across three distances along the fuel bed: 0–3 m, 1–2 m and 2–3 m for burn no. 12 and 5–24 m, 10–20 m and 15–24 m for all other burns. See Table 1 for definitions of variables.

Burn no. – fuel bed	U_5 (m s^{-1})	$U_{0.28}$ (m s^{-1})	Flow type	M_f (% dry mass)	R (m s^{-1})	t_r (s)
1 – A	9.11	7.18	C	12.6	0.24	28
1 – B	9.11	7.18	C	20.4	0.22	27
2 – A	4.59	3.72	C	13.0	0.12	28
2 – B	4.59	3.72	C	15.0	0.11	25
3 – A	9.04	6.72	C	12.8	0.22	24
3 – B	9.04	6.72	C	9.9	0.25	25
4 – A	14.68	10.5	C	6.5	0.72	26
4 – B	14.68	10.5	C	5.2	0.88	23
5 – A	14.71	10.68	RW	6.3	1.06	27
5 – B	14.71	10.68	RW	4.8	0.99	25
6 – A	14.29	10.16	C	9.1	0.59	32
6 – B	14.29	10.16	C	9.3	0.69	29
7 – A	14.09	10.09	C	5.6	0.71	25
7 – B	14.09	10.09	C	5.0	0.60	28
8 – A	10.8	8.24	R	3.4	0.85	24
8 – B	10.8	8.24	R	4.3	0.83	24
9 – A	12.0	8.96	C	6.5	0.58	28
9 – B	12.0	8.96	C	6.7	0.56	26
10 – A	11.7	8.76	C	10.6	0.6	22
10 – B	11.7	8.76	C	5.9	0.74	24
11 – A	11.89	9.17	R	5.8	0.85	25
11 – B	11.89	9.17	R	5.9	0.81	27
12 – A	0.40	0.89	C	7.4	0.01	61
12 – B	0.40	0.89	C	7.4	0.01	52
13 – A	8.67	7.4	R	9.1	0.36	26
13 – B	8.67	7.4	R	8.7	0.28	25
14 – A	10.44	7.74	C	9.4	0.33	24
14 – B	10.44	7.74	C	5.8	0.34	27
15 – A	15.28	12.33	R	8.9	1.01	23
15 – B	15.28	12.33	R	4.4	0.82	16
16 – A	20.75	15.31	C	7.0	1.64	21
16 – B	20.75	15.31	C	7.5	1.73	19
17 – A	26.41	17.58	C	6.6	2.47	15
17 – B	–	–	–	–	–	–

Table 3. Summary statistics of the key measurements for the various datasets used in the analysis

Data shown for each dataset are the mean ± standard deviation and the ranges (in parentheses). See Table 1 for definitions of variables, n is sample size

Dataset	Flow type	n	R (m s^{-1})	U_5 (m s^{-1})	$U_{0.28}$ (m s^{-1})	M_f (% dry mass)	t_r (s)
Full	C	23	0.63 ± 0.59 (0.01–2.47)	11.68 ± 6.07 (0.4–26.41)	8.59 ± 4.08 (0.89–17.58)	8.9 ± 3.8 (5–20.4)	27.8 ± 9.8 (15.0–61.0)
Full	R	8	0.73 ± 0.26 (0.28–1.01)	11.66 ± 2.55 (8.67–15.28)	9.29 ± 2.0 (7.4–12.33)	6.3 ± 2.3 (3.4–9.1)	23.8 ± 3.4 (16.0–27.0)
Full	RW	2	1.02 ± 0.05 (0.99–1.06)	14.71 ± 0 (14.71–14.71)	10.68 ± 0 (10.68–10.68)	5.6 ± 1.1 (4.8–6.3)	26.0 ± 1.41 (25.0–27.0)
Full	All	33	0.67 ± 0.52 (0.01–2.47)	11.86 ± 5.22 (0.40–26.41)	8.89 ± 3.55 (0.89–17.58)	8.1 ± 3.5 (3.4–20.4)	26.7 ± 8.5 (15.0–61.0)
Mod	C	12	0.70 ± 0.71 (0.007–2.467)	12.29 ± 6.80 (0.4–26.41)	8.97 ± 4.49 (0.89–17.58)	8.8 ± 3.4 (5.3–16.5)	27.3 ± 10.0 (15.0–56.5)
ModGr10	C	8	0.98 ± 0.72 (0.34–2.47)	15.54 ± 5.39 (10.44–26.41)	11.14 ± 3.45 (7.74–17.58)	7.1 ± 1.3 (5.3–9.2)	24.0 ± 4.8 (15.0–30.5)
ModLe10	C	4	0.146 ± 0.108 (0.007–0.233)	5.79 ± 4.17 (0.4–9.11)	4.63 ± 2.93 (0.89–7.18)	12.3 ± 3.9 (7.4–16.5)	33.8 ± 15.2 (24.5–56.5)

some experiments in conifer needle litter fuel arrays (Rothermel and Anderson 1966; Catchpole *et al.* 1998; Mendes-Lopes *et al.* 2003). Predictions were made for the range of wind speeds used in model development (original) and the range of wind speeds in the current study (extrapolated). The fine dead fuel moisture contents used to make the predictions were set to equal the average observed during testing (8.1%). For the Catchpole *et al.* (1998) predictions, the fuel bed-dependent constant, fuel particle density and heat of pyrolysis were set to equal the values presented for slash pine needles (Nelson and Adkins 1988).

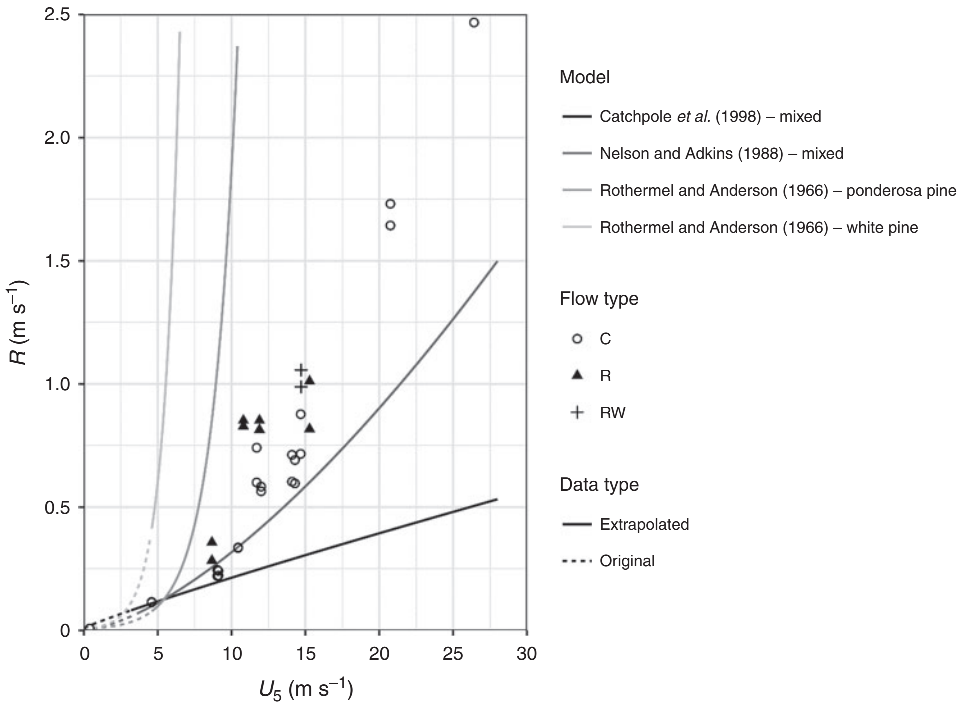

Fig. 2. Observed heading fire rate of spread (R) and wind speed (U_5) from the Insurance Institute for Business & Home Safety (IBHS) full dataset compared with predictions from the rate of spread equations from three laboratory-based studies and their fuel types.

Table 4. Model coefficients and statistics developed to quantify the effect of wind speed and fine dead fuel moisture content on fire rate of spread
P-values are significant at: *, < 0.05; **, < 0.01; and ***, < 0.001. Coefficient standard errors are shown in parentheses. Model fit statistics include the adjusted coefficient of determination for the linear models (R^2), Akaike information criterion (AIC), root mean square error (RMSE) and the mean absolute percent error (MAPE). Note that it is only appropriate to compare AIC values based on models fit using the same dataset. See Table 1 for definitions of variables

Model no.	Equation	Dataset	Intercept (a)	U_5 (b, m s^{-1})	M_f (c, % dry mass)	R^2	AIC	RMSE (m s^{-1})	MAPE (%)
1	1	Full	0.010** (0.003)	1.758*** (0.093)	0.043* (0.019)	–	−30.72	0.135	23.5
2	1	Mod	0.004* (0.002)	1.959*** (0.103)	0.013 (0.026)	–	−18.48	0.080	21.5
3	1	ModGr10	0.004 (0.002)	1.952*** (0.130)	0.011 (0.046)	–	−7.64	0.091	11.5
4	2	Full	−0.209*** (0.152)	0.087*** (0.008)	0.018 (0.011)	0.84	−5.27	0.198	303.9
5	2	Mod	−0.396 (0.338)	0.096*** (0.013)	0.009 (0.026)	0.86	6.80	0.230	555.1
6	2	ModGr10	−1.182* (0.362)	0.133*** (0.01)	0.014 (0.042)	0.96	−4.69	0.109	13.0
7	2	ModLe10	0.0004 (0.000)	0.026*** (0.000)	0.0005* (0.000)	0.99	−56.53	0.000	0.22

For the Nelson and Adkins (1988) predictions, fuel load and residence time were set to the averages obtained in the current study: 0.84 kg m^{-2} and 26.7 s respectively. None of the models presented from previous studies seemed to capture the dependence exhibited by the data from this study at wind speeds exceeding 10 m s^{-1}, likely because of the limited range of wind speeds explored by those studies. The discrepancy between measured and modelled response illustrates the challenges with extrapolating models fit to data from a restricted range to much greater ranges.

Table 4 presents the results of the statistical analysis for the seven models derived from the data. Additionally, Fig. 3 shows the observed versus predicted rate of spread for all seven models. The findings indicated that the effect of wind speed in all models was statistically significant, but the effect of fine dead fuel moisture content was only significant in models 1 and 7. This could be because of low sample size in models 2–6 and/or the limited range of fuel moisture content in the study (mean 8.1%, standard deviation 3.5%, coefficient of variation 43%). The potential problems with analysing small datasets and determining the effects of various experimental factors is well known, particularly in relation to empirical fire spread modelling (Sullivan 2009). However, as in many similar burn experiments, extensive replication is often difficult or impossible because of uncontrollable environmental and logistical constraints.

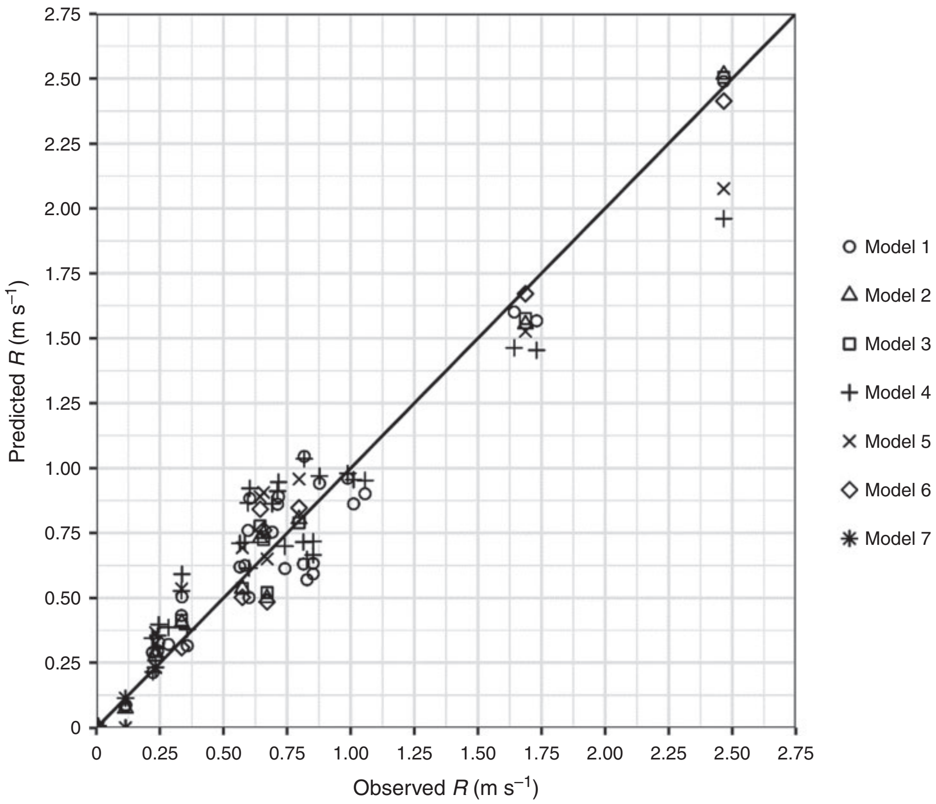

Fig. 3. Observed rate of fire spread versus predictions from each of the seven models of fire rate of spread presented in Table 4.

Sullivan (2009) discusses the implications associated with the value of the wind speed coefficient when using the non-linear model form (Eqn 1). He notes that having a value greater than unity is desirable for dealing with datasets where much of the data are obtained at low wind speeds (i.e. <3 m s^{-1}), but it implies that at some point the rate of spread will exceed the wind speed, which is not realistic. For this reason many models impose a wind limit. The broad collection of power law models assessed by Sullivan (2009) indicated that the median wind function coefficient value was near unity, which is indicative of a linear relationship. Some physical models of fire spread (Grishin *et al.* 1984; Linn *et al.* 2007) also suggest linear relationships between wind speed and the rate of spread. The analysis presented here indicated that over the full range of wind speeds explored the non-linear model form (models 1 and 2), with a wind coefficient of nearly 2, performed better than the linear models (models 4 and 5) with lower AIC, RMSE and MAPE. However, when the dataset was analysed as two separate linear models with a break at U_5 of 10 m s^{-1}, the linear models performed slightly better (Fig. 4).

When considering the findings presented in Table 4 and Fig. 2 at wind speeds less than 10 m s^{-1}, some of the existing models seem to work well (i.e. wind speed slope of Catchpole *et al.* (1998) predictions is 0.021, which is a 2% increase in rate of spread for every unit increase in U_5, which is similar to predictions obtained from Nelson and Adkins (1988)). The linear model fit to the current data (model 7: $U_5 < 10$ m s^{-1}) is 0.026, ~3% increase in the rate of spread for every unit increase in U_5, which is very close to the predictions of Catchpole *et al.* (1998). However, at wind speeds greater than 10 m s^{-1} the existing models tend not to fit the data well and the linear models built using the Full and Mod datasets (i.e. models 4 and 5), significantly under-predict the rate of spread (Fig. 3). At wind speeds greater than 10 m s^{-1} the relationship is linear and stronger than for winds less than 10 m s^{-1}, with the slope of model 6 ($U_5 \geq 10$ m s^{-1}) of 0.133 or a 13% increase in the rate of spread for every unit increase in U_5. When model 6 was used to predict the rate of spread and U_5 was corrected to a 10 m height, the slope was ~12%; that is, the rate of spread was ~12% of the 10-m wind speed, which is close to the 10% rule of thumb (i.e. rate of spread is ~10% of the 10-m wind speed under dry conditions for crown fires and shrubland fires) proposed by Cruz and Alexander (2019).

Effect of flow type

Table 5 presents the ANCOVA results for determining the effect of flow type on the rate of spread (Fig. 2). The assumption of homogeneity of variance and normality of the residuals was met by Leven's test ($P = 0.256$) and the Shapiro–Wilk test ($P = 0.106$), respectively. Flow type was not significant ($P = 0.718$) after accounting for the effects of different wind speeds and dead fine fuel moisture content.

When corrected for differences in average wind speed and fuel moisture content, among the flow types the average rates of

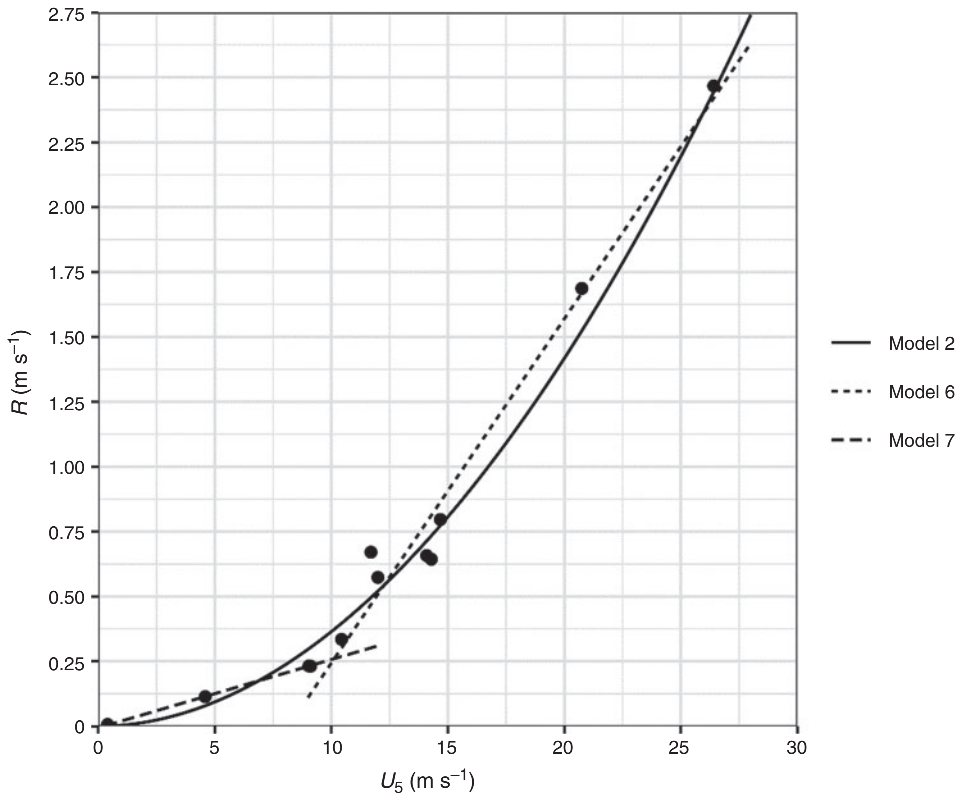

Fig. 4. Scatter plot of observed fire rate of spread (R) and wind speed (U_5) from the Modified (Mod) dataset plotted with predictions from the proposed non-linear model (model 2) and two linear models where $U_5 < 10\ \mathrm{m\ s^{-1}}$ (model 7) and $U_5 \geq 10\ \mathrm{m\ s^{-1}}$ (model 6). Note that the fine dead fuel moisture content was assumed to equal the average for the Mod dataset (i.e. 8.8%).

Table 5. Analysis of covariance results to assess the effect of flow type on fire rate of spread after accounting for the influence of wind speed and fine dead fuel moisture content

See Table 1 for variable definitions

Variable	Degrees of freedom	Sums of squares	Mean square	F value	P value (> F)
U_5 ($\mathrm{m\,s^{-1}}$)	1	7.22	7.22	160.15	<0.001
M_f (% dry mass)	1	0.11	0.11	2.49	0.13
Flow type	2	0.03	0.02	0.34	0.72
Residuals	28	1.26	0.05		

spread for the ‘natural’ wind field fires were not significantly different from those for fires burning under the constant wind conditions over the range of wind speeds in which they overlapped (i.e. $U_5 = 9\text{–}16\ \mathrm{m\,s^{-1}}$). We note that inherent variation in rate of spread because of the experimental setup, small sample size and failure to adequately control the wind speed and fuel moisture factors to the same level during the burns likely hindered the ability to detect a flow-type effect. As depicted in Table 3, although the mean rate of spread was higher for the R and RW flow types, those flow types also had slightly higher average wind speeds and lower fuel moisture content than the C flow type, which after correction resulted in a non-significant effect for this variable. A set of experiments in which wind speed and fuel moisture content are held constant at different levels across the flow types will likely aid in a future analysis to assess the effects of flow type on rate of spread.

Energy release rates

The magnitudes of convective and radiative energy incident at the sensor location respectively varied from 5 to 8 $\mathrm{kW\,m^{-2}}$ at the low wind range and from 60 to 135 $\mathrm{kW\ m^{-2}}$ for the high wind range. Table 6 presents the results of a comparison between the mean levels of convective and radiative heat fluxes at different wind speed levels. Fig. 5 is a scatterplot matrix for the same variables. Both quantities generally responded directly to wind speed with radiative heating increasing approximately

Table 6. Comparison of mean peak radiative and convective heat fluxes across different wind speed groups
Note that the results of the *t*-tests are blank where sample size was inadequate, *n* represents the number of pairs of observations (i.e. radiative and convective fluxes). See Table 1 for variable definitions

U_5 (m s^{-1}) group	*n*	Mean peak radiative flux (kW m^{-2})	Mean peak convective flux (kW m^{-2})	Degrees of freedom	*t* value	*P* value
(0–5)	1	7.6	3.6	–	–	–
(5–10)	1	34.3	7.1	–	–	–
(10–15)	4	73.1	16.9	4.71	4.47	0.01
(15–21)	2	96.6	37.1	1.67	1.40	0.32
All	8	65.9	19.0	10.14	3.07	0.01

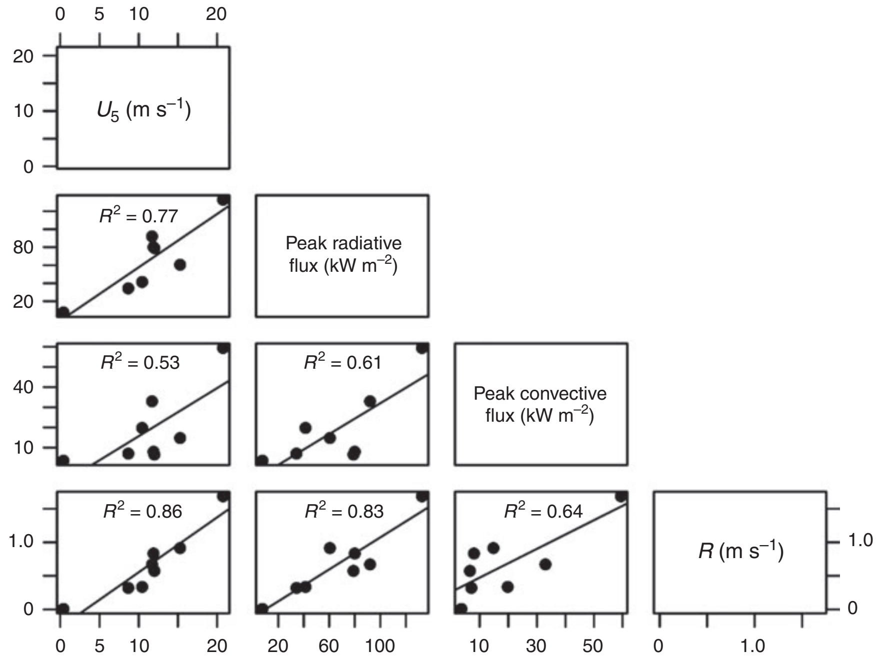

Fig. 5. Scatterplot matrix showing the strength of the linear relationships among wind speed (U_5), fire rate of spread (R), and the peak radiative and convective heat fluxes measured on burns 9–16 (Cleveland 1993). The ordinary least-squares line of best fit is shown, as well as the corresponding coefficient of determination (R^2).

three-fold as much as convective heating over the range of winds explored. A comparison between the ordinary least-squares regression fits of wind speed (independent variable) and heat flux (dependent variable) confirmed that an increase in wind speed had a significantly stronger effect on radiative heating compared with convective heating (*t*-value = 2.22, $P = 0.047$) with coefficients of 5.9 (standard error 1.13) and 2.4 (standard error 1.13) respectively.

Logically, fires burning under low to no wind conditions should be dominated by radiative energy transport whereas fires burning under high wind conditions will exhibit much higher convective heating, possibly on the order of or greater than the radiative heating. Examination of the 10-Hz data from the heat sensors deployed for burns 9–16 showed that on a relatively consistent basis the radiative heating magnitudes were more than twice that of the convective heating. This is in contrast to findings by others that suggest faster response sensors placed at the fuel surface capture short-term convective pulses that exceed the radiative heating magnitudes (Frankman *et al.* 2010, 2013*a*, 2013*b*). The differences between high and low wind fires could also be posited to relate to effective flame emissivity. As winds increase, flame depths are generally deeper; for example, 3-m flame depth has been generally related to an effective emissivity approaching unity in high soot content flames like those characteristic of wildland fires (Àgueda *et al.* 2010; Sudheer and Prabhu 2012).

Fire residence times

Residence time varied from 50 to 60 s at zero winds to less than 20 s for the high winds, with an average residence time of 26.7 s (Fig. 6*a*). Highest residence times were associated with the lowest wind speeds and lowest residence times correlated with highest winds speeds. The general trend indicated a reduction by half for residence time from 0 to 15 m s^{-1} winds followed by an

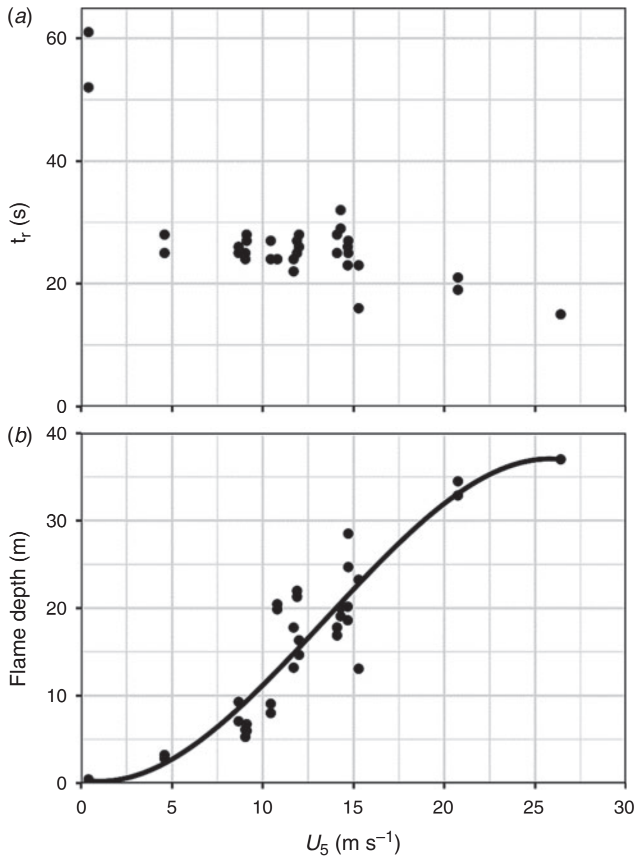

Fig. 6. Measured and calculated flame characteristics for the full Insurance Institute for Business & Home Safety IBHS dataset across increasing wind speeds (U_5), including (*a*) residence time (t_r) and (*b*) flame depth with a 3rd order polynomial line of best fit.

essentially constant residence time. Correlation between wind and residence time has not emerged in other laboratory studies, likely because of limited wind speed capability. Others have explored the relationship between fuel particle size and flame residence time. Burrows (2001) studied the effect of shape, size and arrangement of eucalypt leaves and round wood dowels on flame residence time and reported that particles less than 6 mm in diameter seemed to be the most flammable. Wotton *et al.* (2012) reported an average residence time of 37 s for eucalypt forest fuels, with little dependence on the bulk density or moisture content of the fuel bed. Anderson (1969) reported a minimum residence time of ~60 s for pine needles burned in a quiescent atmosphere, with strong dependence on fuel bed porosity and fuel particle thickness. Catchpole *et al.* (1998) reported residence times from 35 to 66 s for experiments under winds ranging from 0 to 3.2 m s^{-1} at 5 m AGL in fuels and arrangement similar to those reported here. Nelson (2003) presented an analysis of reaction times and burning rates for several datasets. Following his procedure the unit area burning rate for the data from this study ranged from 0.015 to 0.06, which exceeded most of the values presented by Nelson (2003). Furthermore, Nelson (2003) suggested the occurrence of two burning regimens (surface area-controlled and ventilation-controlled) and speculated that the transition between the two correlated with fuel bed porosity. The data here are all at a single porosity value but exhibit a much wider range of surface area burning rates, implying that the type of burning rate regimen could be related to wind as well as fuel bed factors.

Flame depth suggested a strong correlation with wind speed (Fig. 6*b*). Although the nature of the correlation shown implied an upper limit, the data could indeed continue to increase if it were possible to complete the experiments at greater wind speeds. The bulk of the experiments were conducted in the 8–15 m s^{-1} range. It is entirely possible that even higher winds would have led to greater flame depths and lower residence times. Therefore, a secondary finding was the need for further experiments exploring the correlations between flame residence time and flame depth and wind speed beyond the 3 m s^{-1} upper wind speed limit of most wind tunnels.

Conclusions

This work explored the relationship between wind speed and fire rate of spread in fine dead fuels over a wider range of wind speeds than has been investigated in most if not all previously published laboratory studies at this scale. The data suggested a bimodal linear relationship between wind and fire rate of spread, with a break point existing around 10 m s^{-1} indicating lower dependence at winds less than 10 m s^{-1} and higher rate of spread dependence when winds are above that point. As concluded by others (Andrews *et al.* 2013) the data did not exhibit a wind limit, at least up to the maximum wind speed of 27 m s^{-1} explored here. The increased dependency of fire rate of spread as wind exceeds 10 m s^{-1} has implications for both fire behaviour and fire danger rating systems. Radiative heating correlated more strongly with wind speed than convective heating incident on a sensor located slightly above the fuel bed. Flame residence time measurements suggested an inverse correlation with wind speed, at least up to 15 m s^{-1}. Flame depth related directly to wind speed.

Conflicts of interest

The authors have no conflicts of interest.

Acknowledgements

This work was supported through funding provided from the Office of the US Forest Service Deputy Chief for Research. The gracious assistance of the IBHS staff during the experiments is also appreciated as are the comments from the anonymous reviewers.

References

Àgueda AE, Pastor Y, Pérez E, Planas E (2010) Experimental study of the emissivity of flames resulting from the combustion of forest fuels. *International Journal of Thermal Sciences* **49**, 543–554. doi:10.1016/J.IJTHERMALSCI.2009.09.006

Akaike H (1973) Maximum likelihood identification of Gaussian autoregressive moving average models. *Biometrika* **60**, 255–265.

Alexander ME, Stocks BJ, Lawson BD (2000) 'The Canadian forest fire danger rating system'. (Canadian Forest Service: Victoria, BC, Canada)

Anderson HE (1969) Heat transfer and fire spread. USDA Forest Service, Rocky Mountain Research Station. Research Paper INT-RP-69. (Ogden, UT, USA)

Anderson WR, Cruz MG, Fernandes PM, McCaw WL, Vega JA, Bradstock RA, Fogarty L, Gould J, McCarthy G, Marsden-Smedley

JB, Matthews S, Mattingley G, Pearce HG, van Wilgen BW (2015) A generic, empirical-based model for predicting rate of fire spread in shrublands. *International Journal of Wildland Fire* **24**, 443–460. doi:10.1071/WF14130

Andrews P, Bevins C, Seli R (2008) 'BehavePlus fire modeling system'. Version 4.0 user's guide. USDA Forest Service Rocky Mountain Research Station. General Technical Report RMRSGTR-106WWW Revised. (Ogden, UT, USA)

Andrews PL, Cruz MG, Rothermel RC (2013) Examination of the wind speed limit function in the Rothermel surface fire spread model. *International Journal of Wildland Fire* **22**, 959–969. doi:10.1071/WF12122

Beer T (1991) The interaction of wind and fire. *Boundary-Layer Meteorology* **54**, 287–308. doi:10.1007/BF00183958

Beer T (1993) The speed of a fire front and its dependence on wind speed. *International Journal of Wildland Fire* **3**, 193–202. doi:10.1071/WF9930193

Burrows ND (2001) Flame residence times and rates of weight loss of eucalypt forest fuel particles. *International Journal of Wildland Fire* **10**, 137–143. doi:10.1071/WF01005

Butler BW (2014) Wildland firefighter safety zones: a review of past science and summary of future needs. *International Journal of Wildland Fire* **23**, 295–308. doi:10.1071/WF13021

Catchpole WR, Catchpole EA, Butler BW, Rothermel RC, Morris GA, Latham DJ (1998) Rate of spread of free-burning fires in woody fuels in a wind tunnel. *Combustion Science and Technology* **131**, 1–37. doi:10.1080/00102209808935753

Cheney N, Gould J, Catchpole W (1998) Prediction of fire spread in grasslands. *International Journal of Wildland Fire* **8**, 1–13. doi:10.1071/WF9980001

Cleveland WS (1993) 'Visualizing data.' (Hobart Press: Summit, NJ, USA)

Cruz MG, Alexander MW (2019) The 10% wind speed rule of thumb for estimating a wildfire's forward rate of spread in forests and shrublands. *Annals of Forest Science* **76**, 44.

Cruz MG, McCaw WL, Anderson WR, Gould JS (2013) Fire behaviour modelling in semi-arid mallee-heath shrublands of southern Australia. *Environmental Modelling & Software* **40**, 21–34. doi:10.1016/J.ENVSOFT.2012.07.003

Fang JB (1969) An investigation of the effect of controlled wind on the rate of fire spread. PhD Thesis, University of New Brunswick.

Finney MA, Cohen JD, McAllister SS, Jolly WM (2013) On the need for a theory of wildland fire spread. *International Journal of Wildland Fire* **22**, 25–36. doi:10.1071/WF11117

Finney MA, Cohen JD, Forthofer JM, McAllister SS, Gollner MJ, Gorham DJ, Saito K, Akafuah NK, Adam BA, English JD (2015) Role of buoyant flame dynamics in wildfire spread. *Proceedings of the National Academy of Sciences* **112**, 9833–9838.

Frankman D, Webb BW, Butler BW (2010) Time-resolved radiation and convection heat transfer in combusting discontinuous fuel beds. *Combustion Science and Technology* **182**, 1391–1412. doi:10.1080/00102202.2010.486388

Frankman D, Webb BW, Butler B, Jimenez D, Forthofer JM, Sopko P, Shannon KS, Hiers JK, Ottmar RD (2013*a*) Measurements of convective and radiative heating in wildland fires. *International Journal of Wildland Fire* **22**, 157–167. doi:10.1071/WF11097

Frankman D, Webb BW, Butler BW, Jimenez D, Harrington M (2013*b*) The effect of sampling rate on interpretation of the temporal characteristics of radiative and convective heating in wildland flames. *International Journal of Wildland Fire* **22**, 168–173. doi:10.1071/WF12034

Grishin AM, Gruzin AD, Gruzina EE (1984) Aerodynamics and heat exchange between the front of a forest fire and the surface layer of the atmosphere. *Journal of Applied Mechanics* **25**, 889–894.

Levene H (1960) Robust tests for equalify of variances. In 'Contributions to probability and statistics: essays in honor of Harold Hotelling'. Stanford studies in mathematics and statistics 2. (Eds I Olkin, SG Ghurye, W Hoeffding, WG Madow, HB Mann) pp. 278–292. (Stanford University Press: Palo Alto, CA, USA)

Linn R, Winterkamp J, Edminster C, Colman JJ, Smith WS (2007) Coupled influences of topography and wind on wildland fire behaviour. *International Journal of Wildland Fire* **16**, 183–195. doi:10.1071/WF06078

Lopes AMG, Cruz MG, Viegas Zavier D (2002) FireStation: an integrated software system for the numerical simulation of fire spread on complex topography. *Environmental Modelling & Software* **17**, 269–285. doi:10.1016/S1364-8152(01)00072-X

Matthews S (2010) Effect of drying temperature on fuel moisture content measurements. *International Journal of Wildland Fire* **19**, 800–802. doi:10.1071/WF08188

McArthur AG (1966) 'Weather and grassland fire behaviour'. Leaflet no. 100. (Forestry and Timber Bureau: Canberra, ACT, Australia)

McArthur AG (1969) The Tasmanian bushfires of 7 February 1967 and associated fire characteristics. In 'Mass Fire Symposium, Canberra, Australia, 10–12th February, 1969'. (Defence Standards Laboratories: Maribynong, Victoria, Australia)

Mendes-Lopes JMC, Ventura JMP, Amaral JMP (2003) Flame characteristics, temperature–time curves, and rate of spread in fires propagating in a bed of Pinus pinaster needles. *International Journal of Wildland Fire* **12**, 67–84. doi:10.1071/WF02063

Murphy PJ (1963) Rates of fire spread in an artificial fuel. MSc thesis, Montana State University, Bozeman, MT, USA.

Murphy PJ, Beaufait WR, Steele RW (1966) 'Fire spread in an artificial fuel'. Montana Forest and Conservation Experiment Station Bulletin No. 32. (University of Montana: Missoula, MT, USA)

Nelson JRM (2003) Reaction times and burning rates for wind tunnel headfires. *International Journal of Wildland Fire* **12**, 195–211. doi:10.1071/WF02041

Nelson RM, Jr, Adkins CW (1988) A dimensionless correlation for the spread of wind-driven fires. *Canadian Journal of Forest Research* **18**, 391–397. doi:10.1139/X88-058

Potter BE (2012) Atmospheric interactions with wildland fire behaviour – I. Basic surface interactions, vertical profiles and synoptic structures. *International Journal of Wildland Fire* **21**, 779–801. doi:10.1071/WF11128

Rothermel RC (1972) A mathematical model for predicting fire spread in wildland fuels. USDA Forest Service, Intermountain Forest and Range Experiment Station, Research Paper INT-115. (Ogden, UT, USA)

Rothermel RC, Anderson HE (1966) Fire spread characteristics determined in the laboratory. USDA USDA Forest Service, Intermountain Forest and Range Experiment Station, Research Paper INT-30. (Ogden, UT, USA)

Shapiro SS, Wilk MB (1965) An analysis of variance test for normality (complete samples). *Biometrika* **52**, 591–611. doi:10.1093/BIOMET/52.3-4.591

Sharples JJ, McRae RHD, Wilkes SR (2012) Wind–terrain effects on the propagation of wildfires in rugged terrain: fire channelling. *International Journal of Wildland Fire* **21**, 282–296. doi:10.1071/WF10055

Standohar-Alfano CD, Estes H, Johnston T, Morrison MJ, Brown-Giammanco TM (2017) Reducing losses from wind-related natural perils: research at the IBHS Research Center. Frontiers in Built Environment 3, 9. doi:10.3389/FBUIL.2017.00009

Sudheer S, Prabhu SV (2012) Measurement of flame emissivity of hydrocarbon pool fires. *Fire Technology* **48**, 183–217. doi:10.1007/S10694-010-0206-5

Sullivan AL (2009) Wildland surface fire spread modelling, 1990–2007. 1: physical and quasi-physical models. *International Journal of Wildland Fire* **18**, 349–368. doi:10.1071/WF06143

R Development Core Team (2014) R: a language and environment for statistical computing. (R Foundation for Statisticcal Combuting: Vienna, Austria) Available at http://www.R-project.org/ [Verified 3 September 2019]

Weise D (1994) A tilting wind tunnel for fire behavior studies. USDA Forest Service, Pacific Southwest Research Station, Research Note 417. (Albany, CA, USA). doi:10.2737/PSW-RN-417

Weise DR, Biging GS (1996) Effects of wind velocity and slope on flame properties. *Canadian Journal of Forest Research* **26**, 1849–1858. doi:10.1139/X26-210

Willmott CJ (1982) Some comments on the evaluation of model performance. *Bulletin of the American Meteorological Society* **63**, 1309–1313. doi:10.1175/1520-0477(1982)063<1309:SCOTEO>2.0.CO;2

Wotton B, McAlpine R, Hobbs M (1999) The effect of fire front width on surface fire behaviour. *International Journal of Wildland Fire* **9**, 247–253. doi:10.1071/WF00021

Wotton BM, Gould J, McCaw WL, Cheney NP, Taylor SW (2012) Flame temperature and residence time of fires in dry eucalypt forest. *International Journal of Wildland Fire* **21**, 270–281. doi:10.1071/WF10127